

Article

LC/MS-Based Profiling of *Hedyotis aspera* Whole-Plant Methanolic Extract and Evaluation of Its Nephroprotective Potential against Gentamicin-Induced Nephrotoxicity in Rats Supported by In Silico Studies

Dsnbk Prasanth ¹, Lingareddygar Siva Sanker Reddy ², Tharani Dasari ³, Pamula Reddy Bhavanam ⁴, Sheikh F. Ahmad ⁵, Rahul Nalluri ⁶ and Praveen Kumar Pasala ^{7,*}

- ¹ Department of Pharmacognosy, KVSr Siddhartha College of Pharmaceutical Sciences, Vijayawada 520010, Andhra Pradesh, India; dsnbkprasanth@gmail.com
 - ² Department of Pharmaceutical Analysis, Santhiram College of Pharmacy, Nandyal 518112, Andhra Pradesh, India; shiva_s_rl@yahoo.co.in
 - ³ Department of Pharmacology, Santhiram College of Pharmacy, Jawaharlal Nehru Technological University Anantapur, Nandyal 518112, Andhra Pradesh, India; dasaritharani099@gmail.com
 - ⁴ Department of Pharmaceutics, Nirmala College of Pharmacy, Atmakuru, Guntur District, Mangalagiri Mandal 522503, Andhra Pradesh, India; pamula1114@gmail.com
 - ⁵ Department of Pharmacology and Toxicology, College of Pharmacy, King Saud University, Riyadh 11451, Saudi Arabia
 - ⁶ Department of Chemistry, Texas A&M University-Kingsville, Kingsville, TX 78363, USA; rnalluri207@gmail.com
 - ⁷ Department of Pharmacology, Raghavendra Institute of Pharmaceutical Education and Research, Jawaharlal Nehru Technological University Anantapur, Anantapuramu 515721, Andhra Pradesh, India
- * Correspondence: praveenpharmaco@gmail.com



Citation: Prasanth, D.; Reddy, L.S.S.; Dasari, T.; Bhavanam, P.R.; Ahmad, S.F.; Nalluri, R.; Pasala, P.K. LC/MS-Based Profiling of *Hedyotis aspera* Whole-Plant Methanolic Extract and Evaluation of Its Nephroprotective Potential against Gentamicin-Induced Nephrotoxicity in Rats Supported by In Silico Studies. *Separations* **2023**, *10*, 552. <https://doi.org/10.3390/separations10110552>

Academic Editor: Lina Raudonė

Received: 12 October 2023

Revised: 26 October 2023

Accepted: 29 October 2023

Published: 30 October 2023



Copyright: © 2023 by the authors. Licensee MDPI, Basel, Switzerland. This article is an open access article distributed under the terms and conditions of the Creative Commons Attribution (CC BY) license (<https://creativecommons.org/licenses/by/4.0/>).

Abstract: Many high-altitude plants, such as *Hedyotis aspera*, need to be explored for their possible medicinal value. The current study explored the protective effect of *Hedyotis aspera* methanolic extract whole plant (HAME) against gentamicin-induced nephrotoxicity in rats. It profiled their phytocontents using HPLC-QTOF-MS/MS analytic methods. The LC-MS analysis of HAME revealed 27 compounds. Eight compounds followed Lipinski's rule of five and were found to be potential TNF- α inhibitors with binding affinities of -6.9 , -6.3 , -6.3 , and -6.3 Kcal/mol, such as 14,19-Dihydroaspidospermatine, coumeroic acid, lycocernuine and muzanzagenin. All potential compounds were found to be safe according to the ADMET analysis. The in vitro 2,2-diphenyl-1-picrylhydrazyl (DPPH) assay assessed the antioxidant activity. The nephroprotective activity was assessed in rats using a gentamicin-induced nephrotoxicity model. The in vivo analysis involved histological examination, tissue biochemical evaluation, including a kidney function test, catalase activity (CAT), reduced glutathione (GSH) levels, superoxide dismutase (SOD), and the inflammatory mediator TNF- α . Based on DPPH activity, HAME showed a scavenging activity IC_{50} of 264.8 ± 1.2 μ g/mL, while results were compared with a standard vitamin C IC_{50} of 45 ± 0.45 μ g/mL. Nephrotoxicity was successfully induced, as shown by elevated creatinine and uric acid levels, decreased kidney antioxidant levels, and increased TNF- α in gentamicin-treated rats. The HAME treatment significantly reduced serum creatinine and uric acid levels, increased GSH ($p < 0.01$ **), CAT ($p < 0.01$ **), and SOD ($p < 0.001$ ***), and decreased TNF- α ($p < 0.001$ ***) in nephrotoxic rats. The histopathological examination of the groups treated with HAME revealed a notable enhancement in the structural integrity of the kidneys as compared to the group exposed to gentamicin. Biochemical, histopathological, and phytochemical screening of HAME suggests that it has nephroprotective potential, owing to the presence of 14,19-Dihydroaspidospermatine, coumeroic acid, lycopene, and muzanzagenin.

Keywords: *Hedyotis aspera* whole-plant methanolic extract; molecular docking; Wistar rats; nephroprotective effect; gentamicin

1. Introduction

Nephrotoxicity, a prevalent renal illness, might manifest following exposure to a range of frequently utilized drugs and environmental contaminants, potentially resulting in transient or permanent renal impairment [1]. Inflammation and oxidative stress are the two major factors in renal failure [2]. Scientists are now investigating new compounds with potentially protective properties. Animal models, such as aminoglycoside-induced nephrotoxicity models, are now being explored by researchers to study the effects of novel drugs [3]. Gentamicin (GEN) is the most extensively utilized and researched antibiotic within the class of aminoglycosides [4]. The occurrence of nephrotoxicity in patients treated with gentamicin is estimated to be around 13–30% [5]. The gene activation produces reactive oxygen species (ROS), which causes kidney damage [6]. The mechanism causes the formation of hydroxyl radicals and superoxide anions from the kidney mitochondria [7], impairing mitochondrial respiration and cation transport [8].

Plants are increasingly being used for therapeutic purposes worldwide [9]. According to a World Health Organization study, there has been a significant increase in the use of herbal medicines among more than 80% of the population living in poor countries [10]. Scholars have also discovered other phytochemicals and medicinal plants with nephroprotective effects. Gingerol from *Zingiber officinale*, ginsenosides from *Panax ginseng*, crocin from *Crocus sativus*, and quercetin from *Ginkgo biloba* are examples [2].

Hedyotis is a flowering plant genus that belongs to the plant family Rubiaceae. Several species in this genus, notably *Hedyotis biflora*, *Hedyotis corymbosa*, and *Hedyotis diffusa*, are known for their medicinal virtues. *Hedyotis* is native to Asia's tropical and subtropical regions, and the islands of the northwest Pacific [11].

Hedyotis has been reported to have multiple biological activities. Specifically, *H. aspera* has limited pharmacological properties. *Hedyotis diffusa* protects against lipopolysaccharide (LPS)-induced renal inflammation by suppressing proinflammatory cytokine (TNF- α , IL-1 β , IL-6) and chemokine (MCP-1) production, promoting anti-inflammatory cytokine IL-10 production, and protecting renal tissues. Flavonoids and iridoid glycosides are identified as the bioactive constituents present in both serum and renal tissues of mice treated with the *H. diffusa* extract [12]. As per the study by Ying Li et. al., *H. diffusa* extract contains 49 chemicals, and the IL-17 signaling pathway is enriched [13]. MRL/lpr mice improved with HDW: white blood cells, cytokines, autoantibodies, STAT3, IL-17, Ly6G, and MPO reduced in the kidney and neutrophil NETosis was inhibited. HDW reduced urinary protein, inflammatory cells, and glomerular cell proliferation. An aqueous extract was used, and high-dose groups showed reduced urine protein [13]. Based on these previously reported nephroprotective activities, *H. aspera* was selected for the present study.

The major goal of this work was to analyze the phytochemical composition of *Hedyotis aspera* using high-performance liquid chromatography–quadrupole time-of-flight mass spectrometry/mass spectrometry (HPLC-QTOF-MS/MS). The current work used molecular docking techniques to assess the binding affinity of *Hedyotis aspera* phytoconstituents to TNF alpha. The current study aims to evaluate the nephroprotective effects of a methanolic extract obtained from the whole plant of *Hedyotis aspera* against gentamicin (GEN)-induced nephrotoxicity in rats.

2. Materials and Methods

2.1. Collection of Plant Material and Extraction

The *H. aspera* specimen was collected and later identified in the Department of Botany at the Tirumala Hills, Tirupati, Chittoor district, Andhra Pradesh, India. A voucher specimen was deposited at the herbarium and assigned number 0603. Whole plants were then shade-dried, ground, powdered, and extracted with ethanol by maceration. The extract was subsequently dried under a vacuum in a rotary evaporator to produce a crude extract.

2.2. Quantitative Phytochemical Analysis by LC-MS

High-resolution liquid chromatography–mass spectrometry (HR-LC/MS) analysis was performed on the HAME sample using a ChipCube G6550A iFunnel Q-TOF mass spectrometer (Agilent, Santa Clara, CA, USA) equipped with an electrospray ionization source. Phytochemicals were separated using a Hypersil GOLD C-18 column (2.1 × 100 mm, 3 μm particle size) as the stationary phase. The gradient mobile phases of “solvent A” (100% water) and “solvent B” (100% methanol) were used at a flow rate of 300 μL/min. The injection volume of EECL was 3 μL at an injection speed of 100 μL/min with a 5.0 sample flush-out factor. The gradient was started with 95:5 (H₂O/CH₃OH) for 1 min, changed to 0:100 (H₂O/CH₃OH) for 25 min, and returned to 95:5 (H₂O/CH₃CN) for 31 min. The iFunnel MS Q-TOF instrument segment was maintained at a gas flow rate of 13 L/min, a temperature of 250 °C, a gas flow rate of 11 L/min, a sheath gas flow rate of 300 °C, and a nebulizer gas flow pressure of 35 psi. The acquisition method was set to the MS mode with a minimum range of 120 (*m/z*) and a maximum of 1200 (*m/z*), scanning at a rate of 1 spectra/s. The analysis was conducted at the Sophisticated Analytical Instrument Facility (SAIF) of the Indian Institute of Technology, Bombay (IIT Bombay), India [14,15].

2.3. In Silico Studies

2.3.1. Drug-Likeliness

To assess the drug-like properties of the phytoconstituents identified in HAME, a drug-likeness tool (DruLito) was used. DruLito evaluated chemical compounds based on Lipinski’s rule of five, which examines parameters such as the molecular weight, log P, and the number of hydrogen-bond donors and acceptors. This analysis provides insights into the likelihood that the identified phytoconstituents possess drug-like properties [16].

2.3.2. ADMET Analysis

The absorption, distribution, metabolism, excretion, and toxicity (ADMET) prediction tool ADMETSAR was used to evaluate the potential pharmacokinetic properties and toxicity risks associated with the identified phytoconstituents. ADMETSAR utilizes computational models to predict parameters such as aqueous solubility, blood–brain barrier permeability, cytochrome P₄₅₀ inhibition, hepatotoxicity, and mutagenicity. This analysis aids in assessing the overall drug-like characteristics and potential safety concerns of the phytoconstituents. The ADMETSAR results provide valuable insights into the ADME properties and potential risks associated with the identified compounds, guiding further investigations for the development of safe and effective cerebroprotective drugs [17].

2.3.3. Molecular Docking

The docking study was implemented using Auto Dock Vina, and the relevant input files for Auto Dock Vina were generated using the Auto Dock program. TNF-α (PDB ID: 2AZ5) (Figure 1) [18] was used as a target for this study. The RSCB protein data bank provided crystallized structures and PubChem provided 3D structural information on the ligands. Incorporating polar hydrogen atoms and gesture charges is necessary to prepare files through Auto Dock. Table 1 presents the coordinates of the grid box and the grid box size. Vina was implemented using a shell script supplied by Auto Dock Vina developers. The strength of the bond between the ligand and receptor was represented as a negative score (kcal/mol). The AutoDock Vina script produced nine distinct ligand positions with different binding energies for each ligand. A Perl script was used to obtain the ligand with the highest binding affinity for the docked complexes [19].

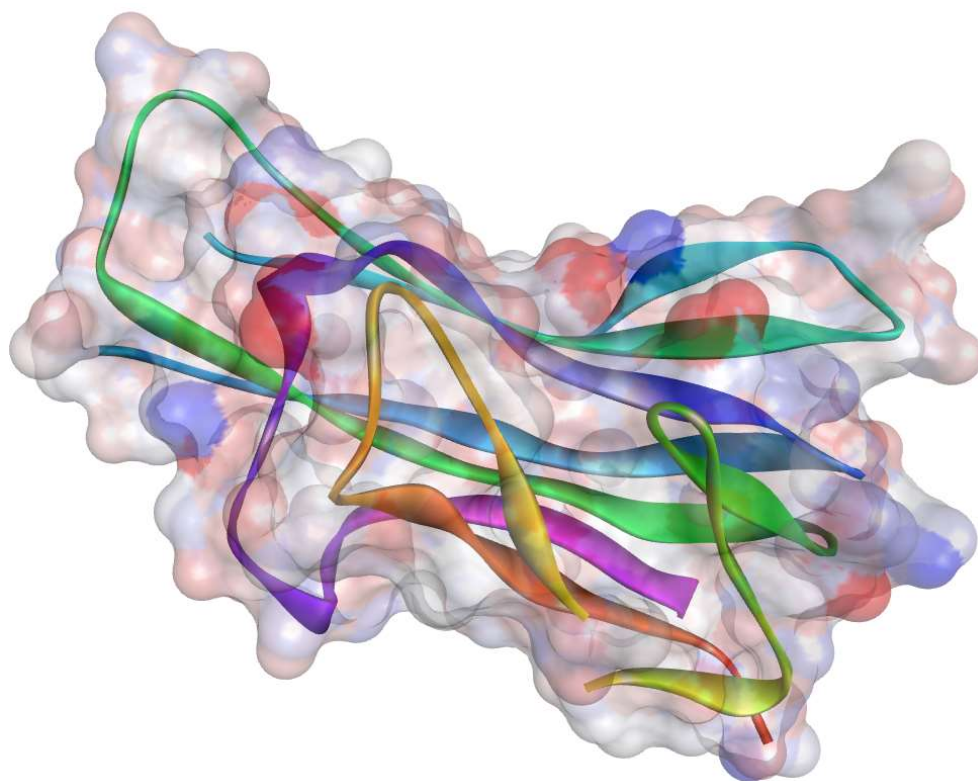


Figure 1. Three-dimensional ribbon-type representation of the crystal structure of TNF- α with a small-molecule inhibitor (PDB: 2AZ5).

Table 1. Molecular docking grid box coordinators used by Auto Dock Vina.

Centre	x	y	z
Tumor necrosis factor (TNF- α)	−19.409600	74.650750	33.849550
Size	x	y	z
Exhaustiveness	10	10	10
	8		

2.4. *In Vitro* Antioxidant Activity by the DPPH Method

The radical scavenging activity was determined using an improved DPPH assay [20]. A volume of 2.7 mL of a 0.2 mM DPPH solution was mixed with 0.3 mL of a different concentration of extract solution. The solution was vigorously agitated before being placed in an incubator at room temperature for one hour, after which the absorbance at 517 nm was measured. Vitamin C concentrations identical to those found in the experimental samples were referred to.

2.5. *The Investigation of Acute Toxicity*

The acute oral toxicity study was carried out by the Organization for Economic Co-operation and Development (OECD) principles, specifically guideline 423, which refers to the Acute Toxic Class Method. HAME was supplied orally via an oral feeding needle at three dosage levels (50, 300, and 2000 mg/kg) [21]. Each dose was administered to a group of three rats. Individual observations of rats were carried out for the first 30 min, followed by targeted monitoring for the next 4 h. After that, daily observations were made for 14 days. The investigation found that, at 2000 mg/kg, the extract had no mortality. For the evaluation of HAME's nephroprotective effects, an LD50 cut-off value of 2500 mg/kg was used, and dosages equivalent to 1/5th (500 mg/kg, p.o.), 1/10th (250 mg/kg, p.o.), and 1/20th (125 mg/kg, p.o.) [22] were chosen.

2.6. Nephroprotective Activity

2.6.1. Experimental Animals

The Wistar rats used in this investigation weighed 200–225 g on average and were obtained from Vyas Lab in Hyderabad, India. These rats were housed and kept in the animal facility at the Santhiram College of Pharmacy in Andhra Pradesh, India. The rats were housed in polypropylene cages under carefully regulated environmental conditions, which included a temperature of 25.2 °C, a relative humidity of 50%, and a 12 h light–dark cycle [23]. All animal-handling protocols have been authorized by the Institutional Review Board (IRB) at Santhiram College of Pharmacy, under permission number 1519/PO/Re/S/11/CPCSEA/2022/006.

2.6.2. Study Design

Animals were randomly divided into four groups, with six animals in each group ($n = 6$).

Negative-control rats served as a normal control and received sodium carboxymethyl cellulose (vehicle for HAME) for 14 days.

Positive-control rats: Served as nephrotoxic controls and received GEN (100 mg/kg/day, i.p.) for 14 days (positive control).

Cystone: standard cystone (100 mg/kg/day, i.p.) and GEN (100 mg/kg/day, i.p.) for 14 days.

HAME (125 mg/kg/day): GEN (100 mg/kg/day, i.p.) and HAME (125 mg/kg/day) were administered orally for 14 days.

HAME (250 mg/kg/day): GEN (100 mg/kg/day, i.p.) and HAME (250 mg/kg/day) were administered orally for 14 days.

HAME (500 mg/kg/day): GEN (100 mg/kg/day, i.p.) and HAME (500 mg/kg/day) were administered orally for 14 days.

The experimental animals were sacrificed 24 h after the last dose of administration and their blood samples and kidneys were collected [24]. The blood samples were centrifuged at 6000 rpm for 10 min at 25 °C, and the serum was used for biochemical analysis.

2.7. Determination of Biomarkers in Kidney

The tissues were processed by homogenizing and mincing them into small pieces (10% *w/v*) using ice-cold 0.1 M phosphate buffer at a pH of 7.4. The resulting solution was then centrifuged for 30 min at 12,000× *g* and 4 °C. The homogenate obtained was used to estimate GSH [25], CAT [26], and SOD [27].

2.8. Determination of Proinflammatory Cytokines

TNF- α concentrations in kidney tissue samples were measured using commercially available kits from R&D Systems, Minneapolis, MN, USA. The sandwich enzyme-linked immunosorbent test (ELISA) was used as the fundamental approach in this work. The absorbance measurement was carried out at a wavelength of 450 nm. The supernatant's protein concentration was measured, and TNF- α levels were quantified and reported as picograms per milligram of protein.

2.9. Histopathological Analysis

After submerging in a 10% neutral-buffered formalin solution, the kidneys were processed and embedded in paraffin wax. Sections were then obtained using a microtome. The sections were stained with hematoxylin and eosin before being examined under a light microscope [28].

2.10. Statistical Analysis

The data were presented as the mean SEM. All data were analyzed using one-tailed *t*-tests and ANOVA (Graphpad Prism 8.0.0). Graphpad prism was used to calculate the IC50 experiments. All in vivo results are shown as mean SEM ($n = 6$) and were analyzed

using a *t*-test followed by ANOVA. The degrees of significance are shown as * $p < 0.05$, ** $p < 0.01$, and *** $p < 0.001$ when compared to the positive (GEN)-control groups.

3. Results

3.1. HR-LC-MS Analysis of HAME

To identify the phytoconstituents, the HAME sample was examined using HR-LC/MS analysis. The retention period, experimental m/z values, MS/MS fragments, discrepancies in the database (library), metabolite class, and suggested chemicals were used as bases for this identification. Positive ionization was used to obtain the mass spectrometry results. The range 226–904 was where the majority of the mass-to-charge (m/z) values were found in the HAME. The chromatogram produced for the HAME assay is shown in Figure 2. Table 2 illustrates the 27 possible phytochemical compounds identified using high-resolution liquid chromatography/mass spectrometry (HR-LC/MS) of the HAME (Figures 2 and 3).

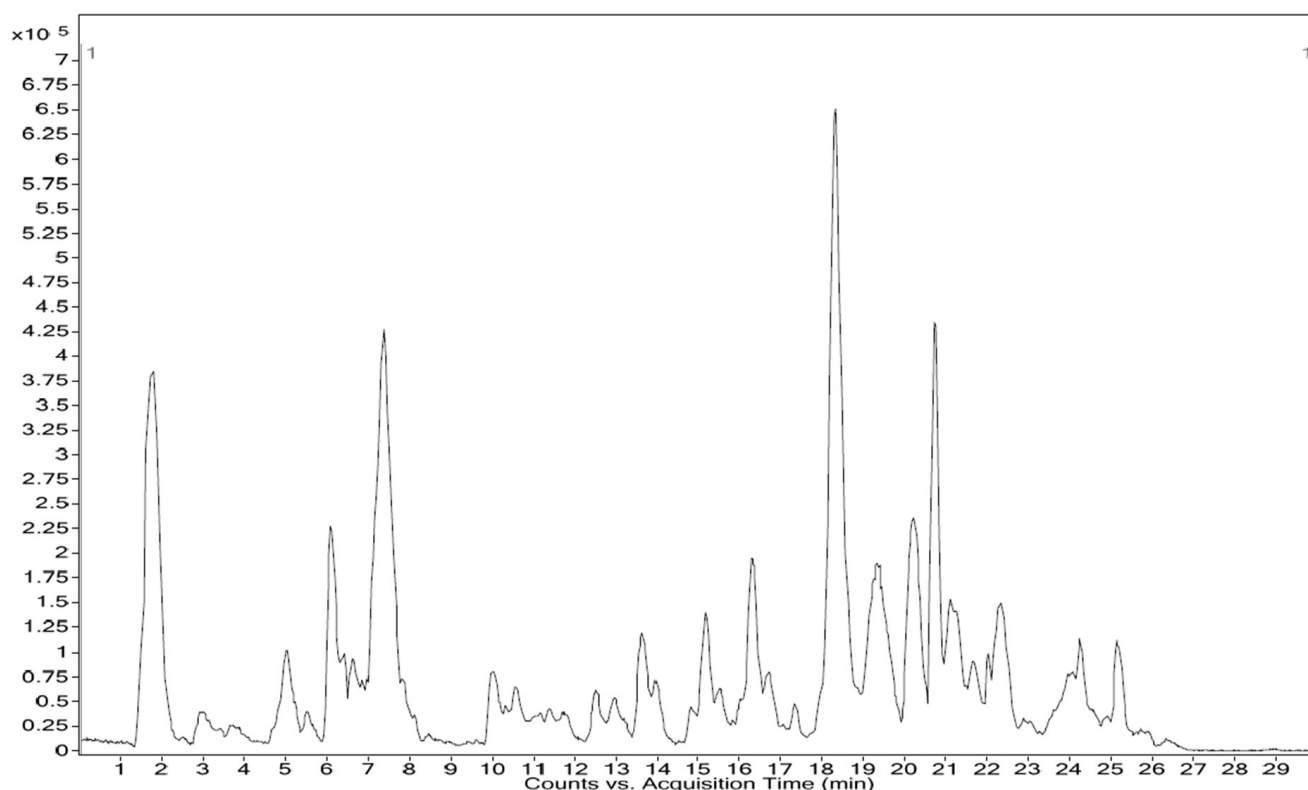


Figure 2. Chromatograms of identified phytochemical constituent profiles in HAME using the HR-LC/MS technique.

Table 2. Phytochemical compounds identified in the HAME using the HR-LC–MS technique.

Name	Formula	Mass	Base Peak	<i>m/z</i>	Start	RT	End	Height	Diff (DB, ppm)
Hellicoside	C ₂₉ H ₃₆ O ₁₇	656.1995	383.1276	701.1998	1.479	1.541	1.602	26,279	−6.5
Fagopyritol B3	C ₂₄ H ₄₂ O ₂₁	666.2295	113.0266	665.2224	1.555	1.555	1.555	15,120	−11.49
Gossypol	C ₃₀ H ₃₀ O ₈	518.1924	101.0261	563.1906	1.528	1.608	1.688	20,437	3.27
1-O-Caffeoyl-(b-D-glucose 6-O-sulfate)	C ₁₅ H ₁₈ O ₁₂ S	422.0554	301.0038	481.0693	1.855	1.925	1.995	15,048	−8.41
Copalliferol B	C ₄₂ H ₃₂ O ₉	680.2041	284.0359	739.218	6.548	6.642	6.736	28,041	0.75
Allivicin	C ₂₇ H ₃₀ O ₁₆	610.1615	300.0322	609.154	6.685	6.775	6.864	66,525	−13.26
Myricitrin	C ₂₁ H ₂₀ O ₁₂	464.103	271.0297	463.0954	6.883	6.957	7.031	55,896	−16.18
Vitisifuran B	C ₅₆ H ₄₀ O ₁₂	904.2379	193.0536	903.231	7.138	7.251	7.363	18,530	15.61
Coumeroic acid	C ₁₇ H ₁₄ N ₂ O ₇	358.075	227.0396	417.0886	7.853	7.934	8.015	16,502	14.29
Glucuheptonic acid	C ₇ H ₁₄ O ₈	226.0676	119.0539	271.0658	9.872	9.964	10.057	14,829	5.47
Makisterone A	C ₂₈ H ₄₆ O ₇	494.3228	503.3426	539.3228	11.271	11.349	11.428	11,939	3.16
Esculentic acid (Phytolacca)	C ₃₀ H ₄₆ O ₆	502.3376	501.3294	501.33	11.876	11.876	11.876	17,037	−16.24
Madasiatic acid	C ₃₀ H ₄₈ O ₅	488.3581	487.3507	487.3508	13.482	13.569	13.656	55,354	−16.2
3-trans-p-Coumaroylrotundic acid	C ₃₉ H ₅₄ O ₇	634.3969	145.033	633.3898	15.726	15.824	15.922	30,116	−15.65
Lansioside B	C ₃₆ H ₅₈ O ₈	618.4027	175.0439	663.4009	16.126	16.126	16.126	11,957	16.93
Ganoderiol I	C ₃₁ H ₅₀ O ₅	502.3741	279.237	501.3668	17.672	17.762	17.852	12,621	−16.57
12-Hydroxy-8,10-octadecadienoic acid	C ₁₈ H ₃₂ O ₃	296.2405	183.0155	295.2332	17.809	17.809	17.809	12,661	−18.05
Ammothamnine	C ₁₅ H ₂₄ N ₂ O ₂	264.1766	183.016	309.1801	19.984	20.076	20.168	63,397	27.16
Bullatetrocin	C ₃₇ H ₆₆ O ₈	638.4821	281.2547	697.4932	20.272	20.272	20.272	15,555	−9.99
9-Oxoasimicinone	C ₃₇ H ₆₄ O ₈	636.4712	152.9989	695.4753	20.402	20.503	20.603	18,698	−17.48
Lamprolobine	C ₁₅ H ₂₄ N ₂ O ₂	264.1753	183.0164	309.1797	21.1	21.191	21.283	36,612	32.09
12,15-cis-Squamostatin A	C ₃₇ H ₆₆ O ₈	638.4814	281.2539	697.4901	21.571	21.571	21.571	17,171	−8.83
Muzanzagenin	C ₂₇ H ₃₈ O ₅	442.2675	441.2621	441.2605	22.129	22.212	22.294	12,469	9.92
Ganoderic acid K	C ₃₂ H ₄₆ O ₉	574.304	445.2131	619.3031	23.291	23.291	23.291	12,520	17.8
14,19-Dihydroaspidospermatine	C ₂₁ H ₂₈ N ₂ O ₂	340.2134	183.0168	339.2065	23.704	23.797	23.89	38,698	4.81
Lycocernuine	C ₁₆ H ₂₆ N ₂ O ₂	278.1978	183.0156	337.2117	24.006	24.097	24.188	55,859	5.76
Santalyl phenylacetate	C ₂₃ H ₃₀ O ₂	338.2118	183.0161	337.2116	25.106	25.207	25.308	17,850	37.86

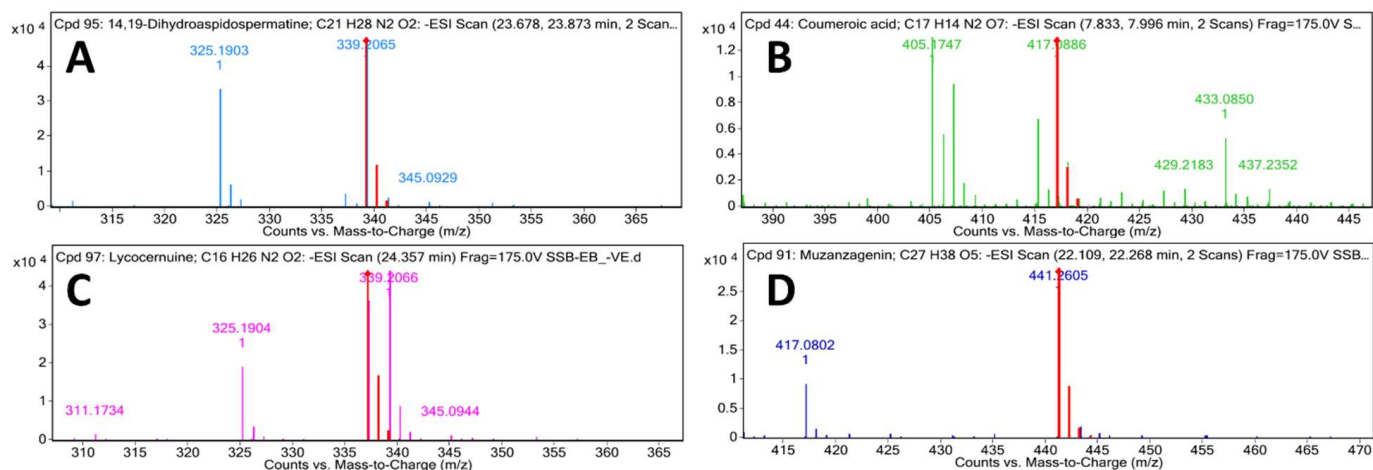


Figure 3. Mass spectral analysis of top-ranked docked compounds against TNF- α eluted from HAME. (A) 14,19-Dihydroaspidospermatine, (B) coumeroyic acid, (C) lycocernuine, and (D) muzanzagenin.

3.2. Drug-Likeliness

The primary aim of this study was to identify potential therapeutic molecules with desirable drug-like properties. The compounds retrieved from the HAME were initially analyzed using DruLito, specifically emphasizing their drug-like characteristics. According to the data obtained from the DruLito server, of a total of 27 compounds, 9 compounds adhered to Lipinski's rule, whereas the remaining 18 compounds did not conform to this rule. The information pertaining to the likelihood of drug use is presented in the accompanying Table 3. The phytochemicals were subsequently subjected to molecular docking analysis to compare their outcomes with those of the standard drug.

3.3. Molecular Docking Studies

This study aimed to gain insight into the binding interactions between phytoconstituents eluted from the HR LC-MS of the HAME and target protein (TNF- α), which is essential in the drug discovery and design process. Specifically, we focused on the binding affinities and interaction profiles of various ligands with TNF- α . To achieve this, we carried out molecular docking studies to determine the binding free energy (ΔG), identify the involved amino acids, and quantify the distances of hydrogen-bond, hydrophobic, and electrostatic interactions for each ligand.

Table 4 displays the binding energies of the eight ligands derived from HAME, which obeyed Lipinski's rule of five. Of the eight compounds, five showed better binding affinity more significant than 8 Kcal/mol. This indicates that HAME has potential compounds that can combat TNF- α . The 2D interactions of ligands with the respective amino acids are presented in the Figure 4, and its 3D interactions were depicted in the Figures 5 and 6.

Table 3. Drug-likeness properties of various compounds eluted from the HR LC-MS of HAME.

Sr. No.	Title	MW	log P	Alog P	HBA	HBD	TPSA	AMR	Violated Lipinski's Rule
1	12,15-cis-Squamostatin A	572	7.914	−8.59	8	0	44.8	140.2	Yes
2	12-Hydroxy-8,10-octadecadienoic acid	264	5.929	−2.07	3	0	17.1	74.92	Yes
3	14,19-Dihydroaspidospermatine	312	2.053	−1.42	4	0	32.8	96.54	No
4	1-O-Caffeoyl-(b-D-glucose 6-O-sulfate)	403.9	−1.72	−1.75	12	0	87.3	92.55	Yes
5	3-trans-p-Coumaroylrotundic acid	580	7.217	1.329	7	0	43.4	181.4	Yes
6	9-Oxoasimicinone	572	7.052	−7.68	8	0	78.9	140.4	Yes
7	Allivicin	579.9	−1.56	−4.86	16	0	63.2	147.2	Yes
8	Ammothamnine	244	0.7	−2.31	2	0	43.4	61.02	No
9	Bullatetrocin	581	8.125	−8.59	8	0	44.8	140.2	Yes
10	Copalliferol B	652	3.242	1.796	9	0	0	213.2	Yes
11	Coumeroic acid	344	1.937	−1.07	9	0	60.4	92.72	No
12	Esculentic acid	459	5.855	0.157	6	0	34.1	137.5	Yes
13	Fagopyritol B3	643	−6.5	−8.31	21	0	55.4	133	Yes
14	Ganoderic acid K	528	1.637	−0.09	9	0	94.6	147.2	Yes
15	Ganoderiol I	457	3.3	1.518	5	0	26.3	144.4	No
16	Glucuheptonic acid	217	−4.41	−3.35	8	0	17.1	44.23	No
17	Gossypol	488	5.944	0.997	8	0	34.1	150.3	Yes
18	Hellicoside	631	−2.17	−3.56	17	0	63.2	157.9	Yes
19	Lamprolobine	242	1.022	−2.18	4	0	40.6	63.73	No
20	Lansioside B	560	7.699	1.781	8	0	35.5	168.8	Yes
21	Lycocernuine	258	1.68	−1.91	4	0	23.6	66.22	No
22	Madasiatic acid	440	6.479	0.495	5	0	17.1	136.8	Yes
23	Makisterone A	455	1.346	−0.78	7	0	17.1	131.8	No
24	Muzanzagenin	412	2.728	0.096	5	0	35.5	119.3	No
25	Myricitrin	449	1.15	−3.4	12	0	44.8	116.4	Yes
26	Santalyl phenylacetate	308	6.143	3.141	2	0	26.3	105.6	Yes
27	Vitisifuran B	863.9	4.767	2.136	12	0	27.7	284.6	Yes

Table 4. Molecular docking of eluted compounds from the HR LC-MS of HAME with TNF- α (PDB:2AZ5).

Compounds	Binding Energies (kcal/mol)
14,19-Dihydroaspidospermatine	−6.9
Coumeroic acid	−6.3
Lycocernuine	−6.3
Muzanzagenin	−6.3
Ammothamnine	−6.1
Ganoderiol I	−5.2
Makisterone A	−5.2
Glucoheptonic acid	−4.6

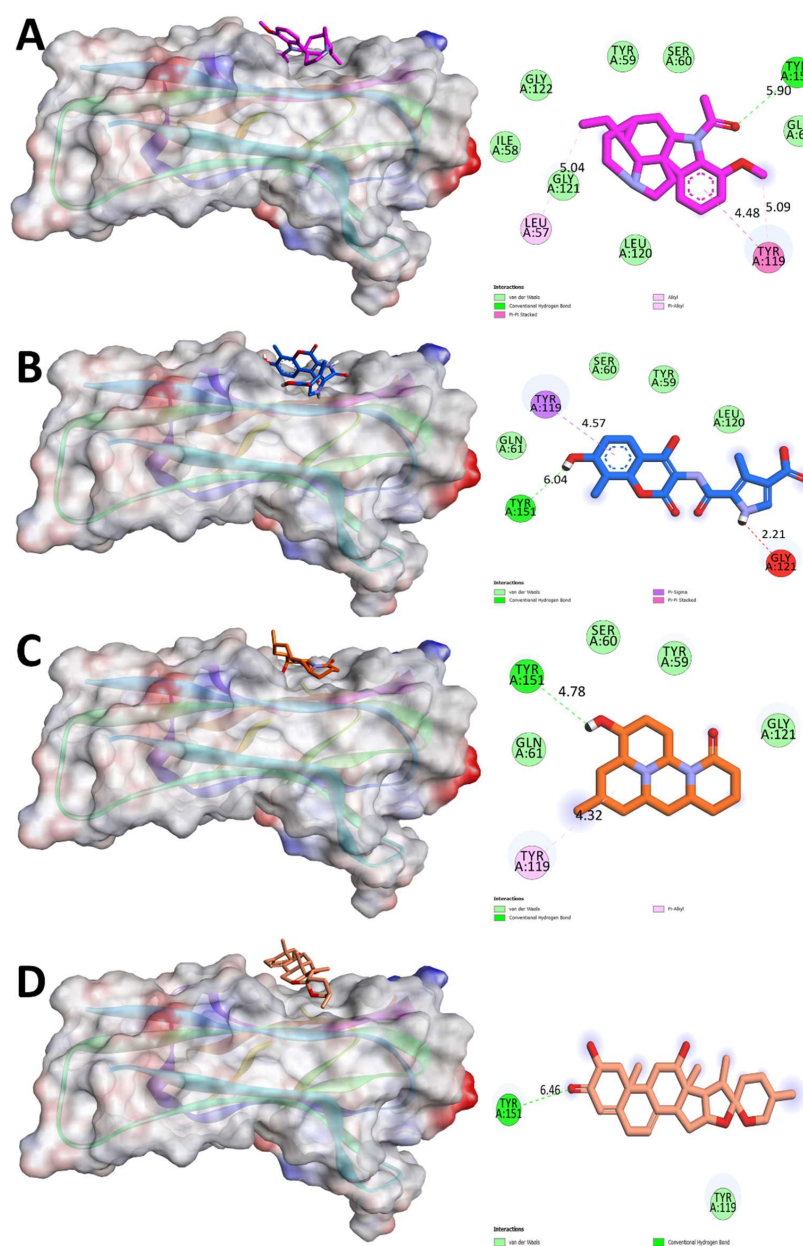


Figure 4. Molecular surface view and 2D representation of phytoconstituents eluted from the HR-LC/MS with TNF- α using the Biovia Drug Discovery Studio 2019. (A) 14,19-Dihydroaspidospermatine, (B) coumeroic acid, (C) lycocernuine, and (D) muzanzagenin.

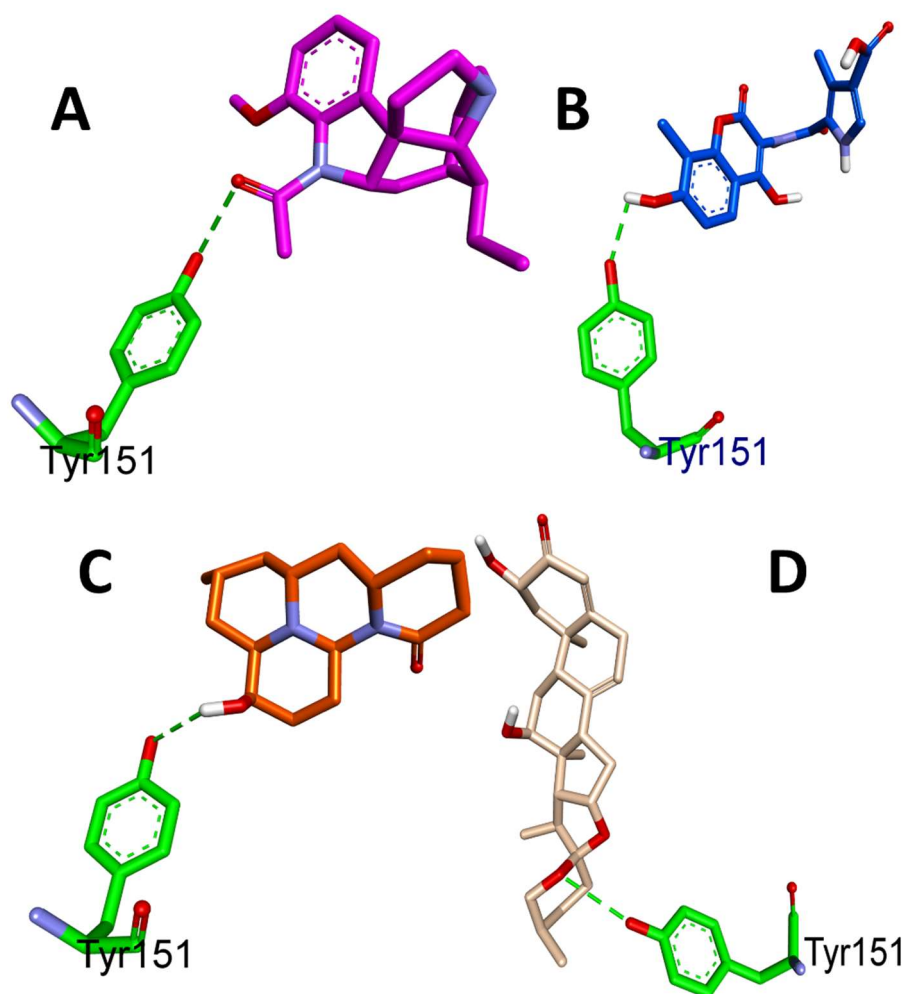


Figure 5. Three-dimensional H-bond interactions of phytocompounds eluted from the HR-LCMS analysis of HAME with TNF- α . (A) 14,19-Dihydroaspidospermatine, (B) coumearic acid, (C) lycocernuine, and (D) muzanzagenin.

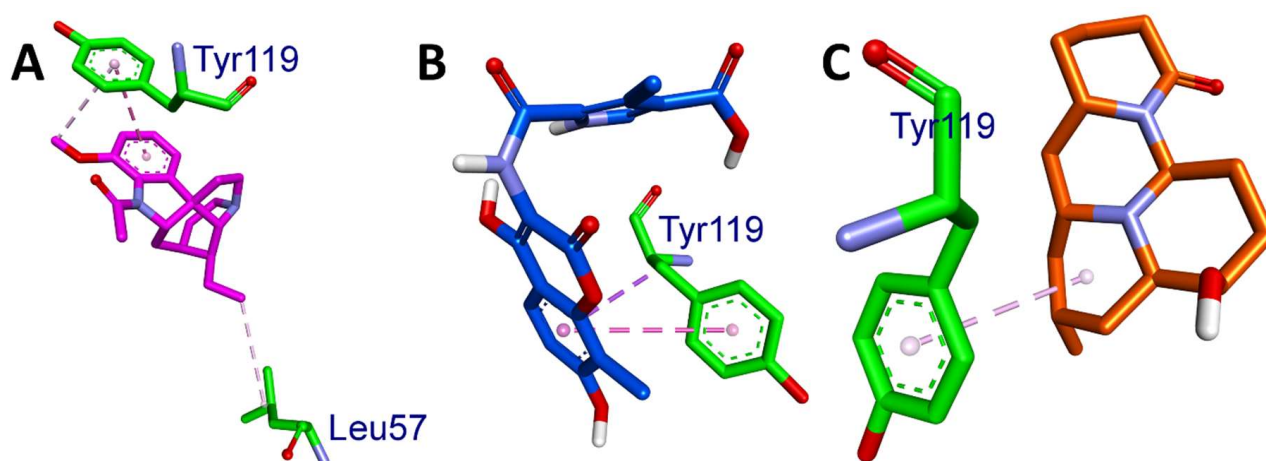


Figure 6. Three-dimensional H-bond interactions of phytocompounds eluted from the HR-LCMS analysis of HAME with TNF- α . (A) 14,19-Dihydroaspidospermatine, (B) coumearic acid, and (C) lycocernuine.

Table 4 shows the binding affinity, ΔG (kcal/mol), of the six ligands to the target protein, as well as the amino acids involved in the binding and the distances between

them. The binding affinity is a measure of the degree to which a ligand binds to a protein. The closer the distance between the amino acids involved in binding, the stronger is the interaction.

The results showed that the binding affinities of the ligands decreased in the following order: 14,19-Dihydroaspidospermatine > coumeroic acid > lycocernuine > muzanzagenin > ammothamnine > ganoderiol I > makisterone A > glucoheptonic acid. This suggests that the binding affinity of the ligands is correlated with the number and strength of interactions between the ligand and protein (Table 5).

Table 5. Binding energies and interaction details of eluted compounds from the HR LC-MS of HAME with TNF- α (PBD: 2AZ5).

Ligands	Binding Affinity, ΔG (Kcal/mol)	Amino Acids Involved and Distance (Å)	
		Hydrogen-Bond Interactions	Hydrophobic Interactions
14,19-Dihydroaspidospermatine	−8.9	TYR A:151 (5.90)	LEU A:57 (5.04), TYR A:119 (4.48, 5.09)
Coumeroic acid	−8.3	TYR A:151 (6.04)	TYR A:119 (6.04)
Lycocernuine	−8.3	TYR A:151 (4.78)	TYR A:119 (4.32)
Muzanzagenin	−8.3	TYR A:151 (6.46)	-
Ammothamnine	−8.1	LEU A:120 (6.87)	-
Ganoderiol I	−5.2	GLN A:61 (4.58), TYR A:151 (6.49)	TYR A:119 (4.14, 5.51), GLY A:121 (4.06)
Makisterone A	−5.2	TYR A:151 (5.12, 5.82), GLY A:121 (4.12)	-
Glucoheptonic acid	−4.6	SER A:60 (4.18), LEU A:120 (4.75), TYR A:151 (5.69, 5.99)	-

Based on the previous study by Nguyen Xuan Ha et al. [29], Tyr151 is one of the amino acid residues located in the active site of the TNF- α dimer protein. All the ligands interacted with Tyr151 through hydrogen bonding, except for ammothamnine. This suggests that these compounds have the potential to inhibit TNF- α activity.

3.4. ADMET Analysis

The ADMET properties of the selected phytochemicals were evaluated using Swiss ADME (<http://www.swissadme.ch/>) accessed on 9 August 2023, admetSAR (<http://lmmd.ecust.edu.cn/admetSAR2/>), accessed on 9 August 2023 and ProTox II (https://tox-new.charite.de/protox_II/) web servers, accessed on 9 August 2023. The predicted ADMET properties of the ligands are listed in Table 6.

To ensure the safety and efficacy of a drug, evaluating its absorption, distribution, metabolism, excretion, and toxicity (ADMET) profile is crucial [30]. This evaluation helps to identify potential issues, such as toxicity, that could result in drug withdrawal from the market. By analyzing these characteristics, researchers can determine whether a compound is likely to be absorbed, distributed, metabolized, and excreted, and whether it causes any harmful effects.

Computational methods for predicting ADMET properties, such as *in silico* forms, have become increasingly popular. These methods offer several advantages over traditional *in vitro* ways, including being faster, cheaper, and potentially more life-saving [31]. *In silico* processes use computer models and algorithms to predict a compound's ADMET properties based on its chemical structure and other relevant factors without animal models. This reduces the time and expenses associated with traditional methods [32].

We evaluated the ADMET profiles of the shortlisted compounds, including drug-likeness, partition coefficients, solubility, HIA, BBB permeability, and cytochrome P450 inhibition (Table 6) [22]. Based on SwissADME, ProTox-ii, and admetSAR, we analyzed the acceptable ADME characteristics, paying particular attention to nontoxicity, as ideal drug candidates [33].

Table 6. ADMET analysis of selected phytoconstituents from the LC-MS analysis of HAME based on molecular docking studies.

Phyto-compounds	Swiss ADME				ADMET SAR										PROTOX-II+				
	log P o/w	Water Solubility	GI Absorption	Lipinski Rule	Veber's Rule	PAINS Alert	TPSA	Lead Likelihood	HIA	CaCO ₂	CYP1A2	CYP2C19	CYP2C9	CYP2D6	LD50 (mg/kg)	Hepato-toxicity	Carcino-genicity	Muta-genicity	Cyto-toxicity
14,19-Dihydroaspidospermatine	3.17	Soluble	High	Yes	Yes	0	32.78	Yes	0.9876	0.7312	0.7957	0.8360	0.7483	0.9308	325 (Class 4)	Inactive	Inactive	Inactive	Inactive
Coumeroic acid	1.25	Soluble	Low	Yes	No	0	152.86	No	0.6350	0.7382	0.9477	0.8825	0.8960	0.9002	1500 (Class 4)	Inactive	Inactive	Inactive	Inactive
Lycocernuine	2.76	Soluble	High	Yes	Yes	0	43.78	Yes	0.9907	0.8063	0.5228	0.6371	0.8185	0.8590	4000 (Class 5)	Inactive	Inactive	Inactive	Inactive
Muzanzagenin	3.64	Soluble	High	Yes	Yes	0	75.99	No	0.9650	0.8957	0.9106	0.9025	0.7898	0.9116	3710 (Class 5)	Inactive	Inactive	Inactive	Inactive

According to the analysis conducted by SwissADME, all four potential compounds complied with Lipinski's rule and possessed good GI absorption, except coumeroic acid. The results of the examination of the predicted PAINS alerts and synthetic accessibility for the medicinal chemistry properties of the drugs (Table 6) showed that all of them had no PAINS alerts (0), indicating that they did not possess any properties that could cause false-positive results in biological assays for the compounds [34].

An essential property of ADMET is its ability to absorb drugs from the human gut (HIA). The ability of drugs to be absorbed from the human gut, known as human intestinal absorption (HIA), is a crucial property of ADMET [35]. HIA plays a pivotal role in the transport of drugs to the target cells [36]. A higher HIA improved the intestinal absorption of the compound [31]. In addition to coumaric acid, all the compounds showed HIA values greater than 0.9, indicating good membrane permeation.

These compounds have been evaluated for their hepatotoxic, carcinogenic, and mutational potential [37]. The analysis of the ProTox II results indicated that all the selected phytoconstituents are safe to use and do not exhibit any hepatotoxicity, carcinogenicity, mutagenicity, or cytotoxicity. These properties are commonly evaluated in ADMET studies to analyze the behavior of drugs [38].

3.5. In Vitro Antioxidant Assay

DPPH is a free-radical compound and has been widely accepted to estimate the scavenging capacity of antioxidants. The DPPH scavenging activities of different concentrations of HAME are presented in Figure 7. HAME showed a scavenging activity IC_{50} of $264.8 \pm 1.2 \mu\text{g/mL}$, while the results were compared with the standard vitamin C IC_{50} of $45 \pm 0.45 \mu\text{g/mL}$.

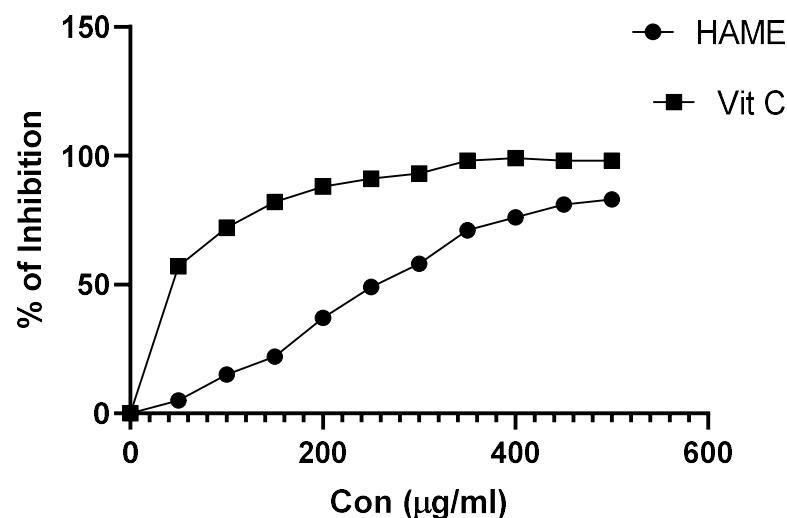


Figure 7. Antioxidant activity of the MAHE as determined by the DPPH method.

3.6. In Vivo Assay

3.6.1. Effect of HAME on Serum Parameters

In the current study, giving GEN (80 mg/kg) for fourteen days resulted in significant nephrotoxicity. This is supported by the data presented in Figure 8, which show a statistically significant increase in serum creatinine levels ($5.11 \pm 0.31 \text{ mg/dL}$, $p < 0.001$ ***), serum uric acid levels ($5.06 \pm 0.39 \text{ mg/dL}$, $p < 0.001$ ***), and blood urea nitrogen levels ($63.86 \pm 0.40 \text{ mg/dL}$, $p < 0.001$ ***). Nonetheless, after the GEN therapy, providing HAME orally at doses of 125 mg/kg, 150 mg/kg, and 300 mg/kg dramatically lowered the levels of these functional indicators, bringing them closer to normal values. The efficacy of HAME increased with increasing dosages of 125 mg/kg, 150 mg/kg, and 300 mg/kg. The maximal dose of HAME resulted in a significant ($p < 0.001$ ***) decrease in blood creatinine levels

(2.45 ± 0.13 mg/dL), uric acid levels (2.52 ± 0.19 mg/dL), and BUN levels (340.41 mg/dL). The ability of HAME to lower blood enzyme levels suggests that they have a protective effect on animal kidneys against GEN's nephrotoxic effects.

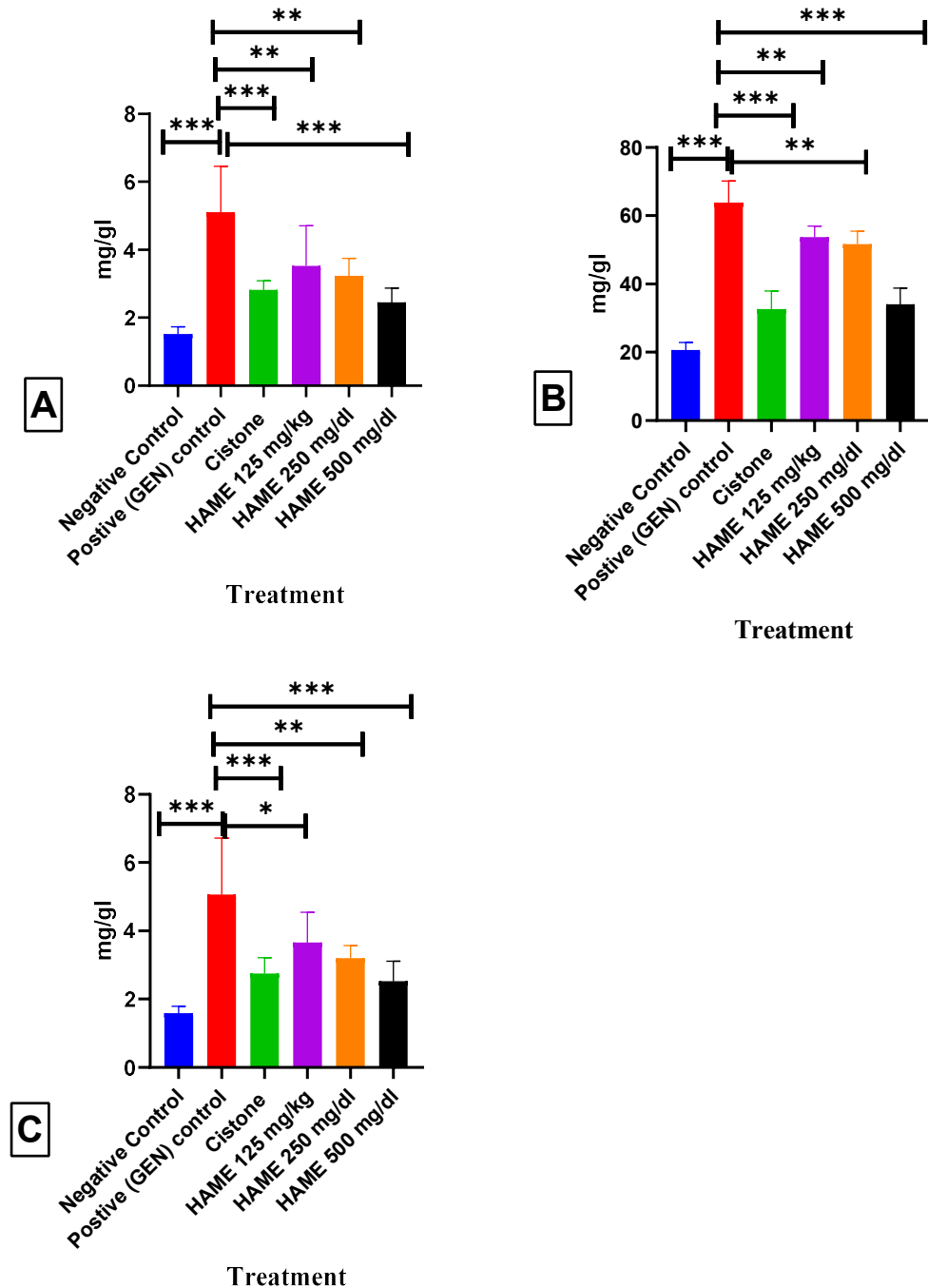


Figure 8. Effect of HAME in serum parameters on GEN-induced nephrotoxicity. (A) Creatinine; (B) Uric acid; (C) Blood urea nitrogen (BUN). The levels of significance calculated by t test are presented as * $p < 0.05$, ** $p < 0.01$, *** $p < 0.001$ compared to the positive (GEN)-control groups.

3.6.2. Effect of HAME on Kidney Antioxidant Parameters

As seen in Figure 9A, a substantial decrease ($p < 0.001$) in SOD levels was observed in rats exposed to GEN compared to the negative-control rats. Conversely, in the groups treated with HAME at three doses (125, 250, and 300 mg/kg), a significant increase

($p < 0.05$ *, $p < 0.001$, and $p < 0.001$, respectively) in SOD levels was observed compared to rats administered with GEN (80 mg/kg; b.w.).

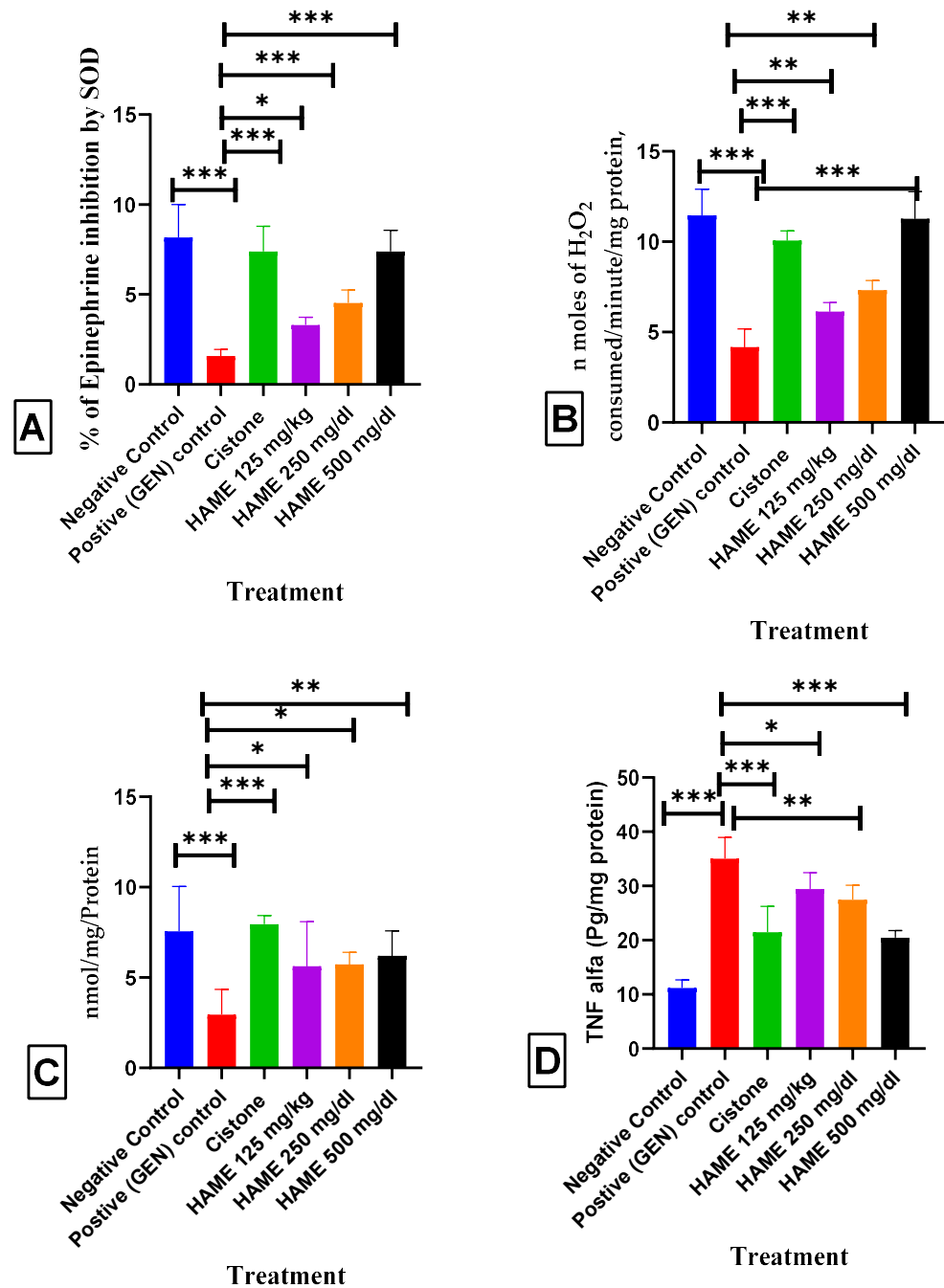


Figure 9. Effect of HAME in kidney tissue parameters on GEN-induced nephrotoxicity. (A) SOD; (B) CAT; (C) GSH; (D) TNF- α . The levels of significance calculated by t test are presented as * $p < 0.05$, ** $p < 0.01$, *** $p < 0.001$ compared to the positive (GEN)-control groups.

As depicted in Figure 9B, a significant decrease ($p < 0.001$) in CAT levels was observed in rats exposed to GEN compared to negative-control rats. Conversely, rats treated with HAME at three doses (125, 250, and 300 mg/kg) showed a significant increase ($p < 0.01$, $p < 0.001$, respectively) in CAT levels compared to rats administered with GEN (80 mg/kg; b.w.).

As shown in Figure 9C, the GSH levels in rats exposed to GEN were significantly decreased ($p < 0.001$) compared to the negative-control rats. However, in the groups treated with HAME at three doses (125, 250, and 300 mg/kg), a significant increase in GSH levels

was observed ($p < 0.05$, $p < 0.01$, and $p < 0.01$, respectively) compared to rats administered with GEN (80 mg/kg; b.w.).

3.6.3. The Impact of HAME on the Expression of TNF- α in the Kidney

TNF- α levels in rats exposed to GEN increased significantly ($p < 0.001$) as compared to rats in the negative-control group, according to the findings shown in Figure 9D. In contrast, when rats were given different doses of HAME (125, 250, and 300 mg/kg), there was a substantial drop in TNF- α levels ($p < 0.05$, $p < 0.01$, and $p < 0.001$, respectively) when compared to rats given GEN at a dose of 80 mg/kg body weight.

3.7. Effect of HAME on Renal Histopathology

The hematoxylin and eosin staining demonstrated that the negative-control group's kidneys exhibited typical renal tubules and glomeruli, as shown in Figure 10A. The rats in the positive-control group had a decrease in glomeruli cells, loss of tubular cell components, atrophy of epithelial cells, deformation of the Bowman space, and deformities in the Bowman's capsule epithelial membrane. In contrast, the negative-control rats (Figure 10A) had normal kidney histoarchitecture. Nonetheless, when the animals were given the HAME extract and then injected with GEN, there was a significant improvement in the histological structure of the kidneys (as seen in Figure 10D–F) compared to the positive (GEN)-control rats (as shown in Figure 10B). Furthermore, the observed improvement in histoarchitecture was comparable to that reported in the negative-control group of rats and the cistone-treated group of rats (Figure 10C).

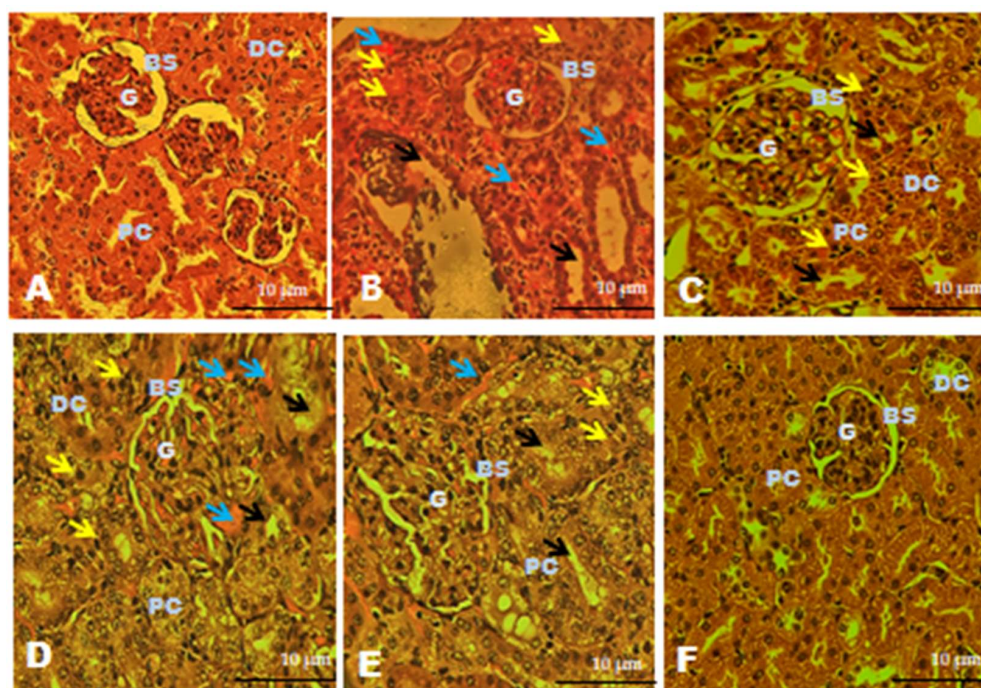


Figure 10. The effect of HAME extracts on kidney histology in GEN-exposed rats. Photomicrographs of the kidney (hematoxylin and eosin staining under a light microscope at 400 magnifications). (A) Negative-control rat, (B) positive (GEN)-control rat, (C) cistone-treated rats, (D) HAME (125 mg/kg), (E) HAME (250 mg/kg), (F) HAME (500 mg/kg) glomerulus (G), distal convoluted tubule (DT), Bowman space (BS), proximal convoluted tubule (PC). Black Arrow Indicates Degeneration and necrosis in renal tubules, Yellow arrow indicates: inflammatory cells infiltration (neutrophils); Blue arrow indicates: inter-tubular hemorrhage.

4. Discussion

The genus *Hedyotis* has many therapeutic characteristics and is used to treat various disorders, including kidney disease. Different plant components are used for their ther-

apeutic properties. The methanolic extract of *Hedyotis aspera* contains several bioactive components. The possible chemicals in this extract were discovered utilizing positive ionization LC-MS and MS/MS analysis. The experimental spectra were compared to in silico fragmentation databases, such as MassBank, HMDB, FooDB, UNPD, KNaPSacK, and NANPDB. These databases are compatible with MS-DIAL and MS-Finder [39].

HR-LC-MS has been widely used in quantitative applications because it has a better level of selectivity and sensitivity than competing techniques [15]. The current study investigated HAME using HR-LC-MS analysis, finding and identifying 27 phytocompounds. These substances were evaluated using Lipinski's rule of five (RO5). Only 8 of the 27 chemical combinations met the RO5 requirements.

The field of drug development has seen considerable growth in the number of methods used. Still, the issue of failed novel compounds due to poor pharmacokinetics or bioavailability remains a significant challenge [40,41]. CADD (computer-aided drug design) is an efficient and time-saving tool that provides an alternative in pharmacology, specifically in silico ADME (absorption, distribution, metabolism, and excretion) analysis, which was conducted in this study to investigate the bioactive compounds of *H. aspera* methanolic extract by predicting a broad range of parameters. All eight compounds were found to be safe as per the ADMET analysis. Molecular docking studies predicted the efficiency of these eight compounds.

The technology of molecular docking is a highly effective method for envisioning the interactions between small-molecule ligands and large-molecule receptors, allowing for identifying potential binding sites and the ligand's geometric configuration. In the present study, a molecular docking technique was utilized to identify the potential phytoconstituents eluted from the HAME capable of suppressing TNF- α activity. Additionally, the investigation aimed to gain deeper insights into the mechanism by which the inhibitor interacts with the protein-binding sites [42]. Structure-based drug discovery is a promising technique for the optimization of lead compounds rapidly and cost-effectively. Molecular docking and dynamics studies were incorporated for the TNF- α target based on the previous studies of Osukoya et al. [43] and Yassir M et al. [44]. The molecular docking studies revealed that 14,19-Dihydroaspidospermatine, coumeroic acid, lycocernuine, and muzanzagenin have the potential to inhibit TNF- α with binding affinities of -6.9 , -6.3 , -6.3 , -6.3 , and -6.3 Kcal/mol, respectively. To the best of our knowledge, this is the first report identifying phytoconstituents in *Hedyotis aspera* by HR-LC/MS analysis. These potential compounds were eluted for the first time, and further in vivo studies are needed to confirm their activity.

The occurrence of nephrotoxicity is a commonly observed adverse outcome associated with chemotherapy treatments in general. The majority of chemotherapy medications selectively focus on pathways that are crucial for the proliferation of cells. [45]. Numerous investigations have provided evidence about the significance of reactive oxygen metabolites in the context of renal injury generated by gentamicin [46]. The nephrotoxicity of drugs is commonly linked to their accumulation in the renal cortex, which is influenced by their affinity for the kidneys and the kinetics of the drug-trapping process [47]. The published literature extensively discusses the nephrotoxicity associated with aminoglycoside antibiotics, with particular emphasis on the widely utilized molecule, gentamicin [48,49]. Multiple investigations have documented the crucial role of oxygen-free radicals as mediators of acute renal failure produced by GEN. Nephrotoxicity generated by genotoxic agents is distinguished by increased concentrations of urea and creatinine in both plasma and urine, together with pronounced proximal tubular necrosis and renal failure [50], and the weights of the kidneys were found to be significantly increased in rats treated with only GEN [51]. Our investigation likewise showed a comparable pattern of alterations subsequent to the administration of GEN. In recent years, numerous studies have demonstrated the potential protective effects of various natural plants against nephrotoxicity generated by GEN [2]. Supplementation of HAME to rats treated with GEN resulted in a reduction in levels of urea, BUN, and creatinine in the serum. These observations suggest that there is an

enhancement in renal function, as seen by the appropriate clearance of urea, blood urea nitrogen (BUN), and creatinine.

Previous research has found that GEN therapy reduces renal SOD, CAT, and GSH activity levels. This decline can be linked to the GM-induced suppression of the endogenous enzymatic antioxidant machinery [52]. HAME treatment effectively reduced the reduction in activity levels of SOD, CAT, and GSH induced by GEN. Several experimental models have demonstrated a link between nephrotoxicity and oxidative stress [53,54].

Previous research has shown that giving GEN can cause renal damage, which activates inflammatory processes and promotes monocyte migration [55]. The control of proinflammatory cytokine release, particularly TNF- α , is critical in renal inflammation during oxidative stress reactions [56]. The current investigation found significant increases in TNF- α concentrations in rats produced by GEN compared to control animals. TNF- α levels in GM rats were significantly lower after HAME administration compared to rats treated with GEN. GEN administration to rats for 14 days caused pathological changes in renal tissue, including decreased cell count in the glomeruli, depletion of cellular tubular components, vascular congestion leading to epithelial cell atrophy, distortions in the Bowman capsule epithelial membrane, and Bowman space deformation. The observed changes in metabolic indicators and tissue damage caused by GEN are consistent with previous observations [57–60]. Nonetheless, regular HAME medication three hours before the GEN injection significantly minimized the unfavorable effects of the GEN. The observed effect of the plant extract was dose-dependent, with the most positive consequence occurring at a dosage of 500 mg/kg.

5. Conclusions

The present investigation has unveiled a wide array of phytochemicals in HAME, with a specific focus on the phytochemicals found in HAME and their potential inhibitory effects on TNF- α . The results of this study indicate that HAME may possess potential nephroprotective properties, necessitating additional investigation to identify the individual phytocompounds responsible for this impact. Four substances, namely, 14,19-Dihydroaspidospermatine, coumerioic acid, lycocernuine, and muzanzagenin, have been recognized as prospective candidates. However, additional investigations are essential to substantiate their efficacy. Based on the findings from biochemical and histological analyses, it may be inferred that the administration of HAME has led to improvements in the changed parameters associated with nephrotoxicity generated by GEN. The obtained results provide preclinical experimental evidence that suggests potential renal protective effects, hence providing support for the extensive use of this botanical remedy in the treatment of kidney ailments. The investigation of the potential protective benefits of HAME against acute kidney injury generated by GM holds significant implications for the advancement of effective treatment approaches for individuals suffering from renal failure.

Author Contributions: Conceptualization, D.P. and P.K.P.; methodology, T.D. and P.K.P.; software, D.P. and S.F.A.; validation, P.K.P.; formal analysis, R.N., L.S.S.R. and S.F.A.; investigation, D.P. and P.K.P.; resources, P.R.B. and P.K.P.; data curation, S.F.A. and T.D.; writing—original draft preparation, T.D., D.P., L.S.S.R. and P.K.P.; writing—review and editing, R.N. and S.F.A.; visualization, D.P., P.R.B. and P.K.P.; supervision, P.K.P. and S.F.A.; project administration, S.F.A.; funding acquisition, S.F.A. All authors have read and agreed to the published version of the manuscript.

Funding: This research was funded by King Saud University, Riyadh, Saudi Arabia, project number (RSPD2023R709).

Data Availability Statement: The data presented in this study are available on request from the corresponding author.

Acknowledgments: The authors acknowledge and extend their appreciation to the Researchers Supporting Project Number (RSPD2023R709), King Saud University, Riyadh, Saudi Arabia for funding this study.

Conflicts of Interest: The authors declare no conflict of interest.

References

1. El-Tantawy, W.H.; Mohamed, S.A.; Abd Al Haleem, E.N. Evaluation of biochemical effects of Casuarina equisetifolia extract on gentamicin-induced nephrotoxicity and oxidative stress in rats. *Phytochemical analysis. J. Clin. Biochem. Nutr.* **2013**, *53*, 158–165. [[CrossRef](#)]
2. Boozari, M.; Hosseinzadeh, H. Natural medicines for acute renal failure: A review. *Phytother. Res.* **2017**, *31*, 1824–1835. [[CrossRef](#)] [[PubMed](#)]
3. Casanova, A.G.; Vicente-Vicente, L.; Hernandez-Sanchez, M.T.; Pescador, M.; Prieto, M.; Martinez-Salgado, C.; Morales, A.I.; Lopez-Hernandez, F.J. Key role of oxidative stress in animal models of aminoglycoside nephrotoxicity revealed by a systematic analysis of the antioxidant-to-nephroprotective correlation. *Toxicology* **2017**, *385*, 10–17. [[CrossRef](#)] [[PubMed](#)]
4. Kopple, J.D.; Ding, H.; Letoha, A.; Ivanyi, B.; Qing, D.P.; Dux, L.; Wang, H.Y.; Sonkodi, S. L-carnitine ameliorates gentamicin-induced renal injury in rats. *Nephrol. Dial. Transplant.* **2002**, *17*, 2122–2131. [[CrossRef](#)]
5. Mathew, T.H. Drug-induced renal disease. *Med. J. Aust.* **1992**, *156*, 724–728. [[CrossRef](#)] [[PubMed](#)]
6. Qadir, M.I.; Tahir, M.; Lone, K.P.; Munir, B.; Sami, W. Protective role of ginseng against gentamicin induced changes in kidney of albino mice. *J. Ayub Med. Coll. Abbottabad* **2011**, *23*, 53–57.
7. Walker, P.D.; Barri, Y.; Shah, S.V. Oxidant Mechanisms in Gentamicin Nephrotoxicity. *Ren. Fail.* **1999**, *21*, 433–442. [[CrossRef](#)]
8. Doroshov, J.H.; Davies, K.J. Redox cycling of anthracyclines by cardiac mitochondria. II. Formation of superoxide anion, hydrogen peroxide, and hydroxyl radical. *J. Biol. Chem.* **1986**, *261*, 3068–3074. [[CrossRef](#)]
9. Hussain, K.; Nisar, M.F.; Majeed, A.; Nawaz, K.; Bhatti, K.H. Ethnomedicinal survey for important plants of Jalalpur Jattan, district Gujrat, Punjab, Pakistan. *Ethnobot. Leaflet* **2010**, *2010*, 11.
10. Ghatapanadi, S.; Johnson, N.; Rajasab, A. *Documentation of Folk Knowledge on Medicinal Plants of Gulbarga District, Karnataka*; NISCAIR-CSIR: New Delhi, India, 2011.
11. Mabberley, D.J. *Mabberley's Plant-Book: A Portable Dictionary of Plants, Their Classification and Uses*; Cambridge University Press: Cambridge, UK, 2017.
12. Ye, J.-H.; Liu, M.-H.; Zhang, X.-L.; He, J.-Y. Chemical Profiles and Protective Effect of *Hedyotis diffusa* Willd in Lipopolysaccharide-Induced Renal Inflammation Mice. *Int. J. Mol. Sci.* **2015**, *16*, 27252–27269. [[CrossRef](#)]
13. Li, Y.; Ding, T.; Chen, J.; Ji, J.; Wang, W.; Ding, B.; Ge, W.; Fan, Y.; Xu, L. The protective capability of *Hedyotis diffusa* Willd on lupus nephritis by attenuating the IL-17 expression in MRL/lpr mice. *Front. Immunol.* **2022**, *13*, 943827. [[CrossRef](#)]
14. Noumi, E.; Snoussi, M.; Anouar, E.H.; Alreshidi, M.; Veetil, V.N.; Elkahoui, S.; Adnan, M.; Patel, M.; Kadri, A.; Aouadi, K.; et al. HPLC-based metabolite profiling, antioxidant, and anticancer properties of *Teucrium polium* L. Methanolic extract: Computational and in vitro study. *Antioxidants* **2020**, *9*, 1089. [[CrossRef](#)] [[PubMed](#)]
15. Singh, P.K.; Singh, J.; Medhi, T.; Kumar, A. Phytochemical Screening, Quantification, FT-IR Analysis, and In Silico Characterization of Potential Bio-active Compounds Identified in HR-LC/MS Analysis of the Polyherbal Formulation from Northeast India. *ACS Omega* **2022**, *7*, 33067–33078. [[CrossRef](#)] [[PubMed](#)]
16. Setlur, A.S.; Naik, S.Y.; Skariyachan, S. Herbal Lead as Ideal Bioactive Compounds Against Probable Drug Targets of Ebola Virus in Comparison with Known Chemical Analogue: A Computational Drug Discovery Perspective. *Interdiscip. Sci.* **2017**, *9*, 254–277. [[CrossRef](#)] [[PubMed](#)]
17. Prasanth, D.; Panda, S.P.; Rao, A.L.; Chakravarti, G.; Teja, N.; Vani, V.B.N.; Sandhya, T. In-silico strategies of some selected phytoconstituents from zingiber officinale as SARS CoV-2 main protease (COVID-19) inhibitors. *Indian J. Pharm. Educ. Res.* **2020**, *54*, s552–s559. [[CrossRef](#)]
18. Lin, S.H.; Huang, K.J.; Weng, C.F.; Shiu, D. Exploration of natural product ingredients as inhibitors of human HMG-CoA reductase through structure-based virtual screening. *Drug Des. Dev. Ther.* **2015**, *9*, 3313–3324. [[CrossRef](#)]
19. Sharma, V.; Pattanaik, K.K.; Jayprakash, V.; Basu, A.; Mishra, N. A utility script for automating and integrating AutoDock and other associated programs for virtual screening. *Bioinformation* **2009**, *4*, 84–86. [[CrossRef](#)] [[PubMed](#)]
20. Huang, B.; Ban, X.; He, J.; Tong, J.; Tian, J.; Wang, Y. Hepatoprotective and antioxidant activity of ethanolic extracts of edible lotus (*Nelumbo nucifera* Gaertn.) leaves. *Food Chem.* **2010**, *120*, 873–878. [[CrossRef](#)]
21. Jonsson, M.; Jestoi, M.; Nathanail, A.V.; Kokkonen, U.-M.; Anttila, M.; Koivisto, P.; Karhunen, P.; Peltonen, K. Application of OECD Guideline 423 in assessing the acute oral toxicity of moniliformin. *Food Chem. Toxicol.* **2013**, *53*, 27–32. [[CrossRef](#)]
22. Govindappa, P.K.; Gautam, V.; Tripathi, S.M.; Sahni, Y.P.; Raghavendra, H.L.S. Effect of *Withania somnifera* on gentamicin induced renal lesions in rats. *Rev. Bras. Farm.* **2019**, *29*, 234–240. [[CrossRef](#)]
23. Chaware, V.; Chaudhary, B.; Vaishnav, M.; Biyani, K. Protective effect of the aqueous extract of *Momordica charantia* leaves on gentamicin induced nephrotoxicity in rats. *Int. J. PharmTech Res.* **2011**, *3*, 553–555.
24. Lakshmi, B.; Sudhakar, M. Protective effect of *Zingiber officinale* on gentamicin-induced nephrotoxicity in rats. *IJP-Int. J. Pharmacol.* **2010**, *6*, 58–62. [[CrossRef](#)]
25. Sedlak, J.; Lindsay, R.H. Estimation of total, protein-bound, and nonprotein sulfhydryl groups in tissue with Ellman's reagent. *Anal. Biochem.* **1968**, *25*, 192–205. [[CrossRef](#)]
26. Aebi, H. Catalase in vitro. In *Methods in Enzymology*; Elsevier: Amsterdam, The Netherlands, 1984; Volume 105, pp. 121–126.

27. Marklund, S.; Marklund, G. Involvement of the superoxide anion radical in the autoxidation of pyrogallol and a convenient assay for superoxide dismutase. *Eur. J. Biochem.* **1974**, *47*, 469–474. [[CrossRef](#)]
28. Cardiff, R.D.; Miller, C.H.; Munn, R.J. Manual hematoxylin and eosin staining of mouse tissue sections. *Cold Spring Harb. Protoc.* **2014**, *2014*, pdb-prot073411. [[CrossRef](#)] [[PubMed](#)]
29. Ha, N.X.; Anh, H.T.N.; Khanh, P.N.; Ha, V.T.; Ha, N.V.; Huong, T.T.; Cuong, N.M. In silico and ADMET study of Morinda longissima phytochemicals against TNF- α for treatment of inflammation-mediated diseases. *Vietnam. J. Chem.* **2023**, *61*, 57–63.
30. Ferreira, L.L.G.; Andricopulo, A.D. ADMET modeling approaches in drug discovery. *Drug Discov. Today* **2019**, *24*, 1157–1165. [[CrossRef](#)] [[PubMed](#)]
31. Killari, K.N.; Polimati, H.; Prasanth, D.; Singh, G.; Panda, S.P.; Vedula, G.S.; Tatipamula, V.B. Salazinic acid attenuates male sexual dysfunction and testicular oxidative damage in streptozotocin-induced diabetic albino rats. *RSC Adv.* **2023**, *13*, 12991–13005. [[CrossRef](#)]
32. Norinder, U.; Bergstrom, C.A. Prediction of ADMET Properties. *ChemMedChem* **2006**, *1*, 920–937. [[CrossRef](#)]
33. Bickerton, G.R.; Paolini, G.V.; Besnard, J.; Muresan, S.; Hopkins, A.L. Quantifying the chemical beauty of drugs. *Nat. Chem.* **2012**, *4*, 90–98. [[CrossRef](#)]
34. Olasupo, S.B.; Uzairu, A.; Shallangwa, G.A.; Uba, S. Unveiling novel inhibitors of dopamine transporter via in silico drug design, molecular docking, and bioavailability predictions as potential antischizophrenic agents. *Future J. Pharm. Sci.* **2021**, *7*, 63. [[CrossRef](#)]
35. Pardridge, W.M. The Blood-Brain Barrier: Bottleneck in Brain Drug Development. *Neurotherapeutics* **2005**, *2*, 3–14. [[CrossRef](#)]
36. Ejeh, S.; Uzairu, A.; Shallangwa, G.A.; Abechi, S.E. In silico design, drug-likeness and ADMET properties estimation of some substituted thienopyrimidines as HCV NS3/4A protease inhibitors. *Chem. Afr.* **2021**, *4*, 563–574. [[CrossRef](#)]
37. Lounkine, E.; Keiser, M.J.; Whitebread, S.; Mikhailov, D.; Hamon, J.; Jenkins, J.L.; Lavan, P.; Weber, E.; Doak, A.K.; Cote, S.; et al. Large-scale prediction and testing of drug activity on side-effect targets. *Nature* **2012**, *486*, 361–367. [[CrossRef](#)]
38. Pantaleão, S.Q.; Fernandes, P.O.; Gonçalves, J.E.; Maltarollo, V.G.; Honorio, K.M. Recent advances in the prediction of pharmacokinetics properties in drug design studies: A review. *ChemMedChem* **2022**, *17*, e202100542. [[CrossRef](#)] [[PubMed](#)]
39. Kim, J.; Lee, K.P.; Kim, M.-R.; Kim, B.S.; Moon, B.S.; Shin, C.H.; Baek, S.; Hong, B.S. A network pharmacology approach to explore the potential role of Panax ginseng on exercise performance. *Phys. Act. Nutr.* **2021**, *25*, 28. [[CrossRef](#)]
40. Han, C.; Wang, B. Factors that impact the developability of drug candidates: An overview. *Drug Deliv. Princ. Appl.* **2005**, 1–14. [[CrossRef](#)]
41. Waring, M.J.; Arrowsmith, J.; Leach, A.R.; Leeson, P.D.; Mandrell, S.; Owen, R.M.; Pairaudeau, G.; Pennie, W.D.; Pickett, S.D.; Wang, J. An analysis of the attrition of drug candidates from four major pharmaceutical companies. *Nat. Rev. Drug Discov.* **2015**, *14*, 475–486. [[CrossRef](#)]
42. Al-Rajhi, A.M.H.; Qanash, H.; Almashjary, M.N.; Hazzazi, M.S.; Felemban, H.R.; Abdelghany, T.M. Anti-*Helicobacter pylori*, Antioxidant, Antidiabetic, and Anti-Alzheimer's Activities of Laurel Leaf Extract Treated by Moist Heat and Molecular Docking of Its Flavonoid Constituent, Naringenin, against Acetylcholinesterase and Butyrylcholinesterase. *Life* **2023**, *13*, 1512. [[CrossRef](#)] [[PubMed](#)]
43. Osukoya, O.A.; Oyinloye, B.E.; Ajiboye, B.O.; Olokode, K.A.; Adeola, H.A. Nephroprotective and anti-inflammatory potential of aqueous extract from *Persea americana* seeds against cadmium-induced nephrotoxicity in Wistar rats. *Biomaterials* **2021**, *34*, 1141–1153. [[CrossRef](#)] [[PubMed](#)]
44. Yassir, M.; Tir, M.; Mufti, A.; Feriani, A.; Faidi, B.; Tlili, N.; Sobeh, M. *Millettia ferruginea* extract attenuates cisplatin-induced alterations in kidney functioning, DNA damage, oxidative stress, and renal tissue morphology. *Arab. J. Chem.* **2022**, *15*, 104037. [[CrossRef](#)]
45. Hanigan, M.H.; Devarajan, P. Cisplatin nephrotoxicity: Molecular mechanisms. *Cancer Ther.* **2003**, *1*, 47.
46. Ueda, N.; Kaushal, G.P.; Shah, S.V. Apoptotic mechanisms in acute renal failure. *Am. J. Med.* **2000**, *108*, 403–415. [[CrossRef](#)]
47. Karahan, İ.; Ateşşahin, A.; Yılmaz, S.; Çeribaşı, A.; Sakin, F. Protective effect of lycopene on gentamicin-induced oxidative stress and nephrotoxicity in rats. *Toxicology* **2005**, *215*, 198–204. [[CrossRef](#)]
48. Cuzzocrea, S.; Mazzon, E.; Dugo, L.; Serraino, I.; Di Paola, R.; Britti, D.; De Sarro, A.; Pierpaoli, S.; Caputi, A.P.; Masini, E. A role for superoxide in gentamicin-mediated nephropathy in rats. *Eur. J. Pharmacol.* **2002**, *450*, 67–76. [[CrossRef](#)] [[PubMed](#)]
49. Al-Majed, A.A.; Mostafa, A.M.; Al-Rikabi, A.C.; Al-Shabanah, O.A. Protective effects of oral arabic gum administration on gentamicin-induced nephrotoxicity in rats. *Pharmacol. Res.* **2002**, *46*, 445–451. [[CrossRef](#)] [[PubMed](#)]
50. Erdem, A.; Gündogan, N.Ü.; Usubütün, A.; Kılınc, K.; Erdem, R.N.; Kara, A.; Bozkurt, A. The protective effect of taurine against gentamicin-induced acute tubular necrosis in rats. *Nephrol. Dial. Transplant.* **2000**, *15*, 1175–1182. [[CrossRef](#)]
51. Harlalka, G.V.; Patil, C.R.; Patil, M.R. Protective effect of *Kalanchoe pinnata* pers. (*Crassulaceae*) on gentamicin-induced nephrotoxicity in rats. *Indian J. Pharmacol.* **2007**, *39*, 201. [[CrossRef](#)]
52. Thounaojam, M.C.; Jadeja, R.N.; Devkar, R.V.; Ramachandran, A. Sida rhomboidea. Roxb leaf extract ameliorates gentamicin induced nephrotoxicity and renal dysfunction in rats. *J. Ethnopharmacol.* **2010**, *132*, 365–367. [[CrossRef](#)] [[PubMed](#)]
53. Arunkumar, P.; Viswanatha, G.; Radheshyam, N.; Mukund, H.; Belliyappa, M. Science behind cisplatin-induced nephrotoxicity in humans: A clinical study. *Asian Pac. J. Trop. Biomed.* **2012**, *2*, 640–644. [[CrossRef](#)]
54. Neeraj, K.G.; Sharad, M.; Tejram, S.; Abhinav, M.; Suresh, P.V.; Rajeev, K.T. Evaluation of anti-apoptotic activity of different dietary antioxidants in renal cell carcinoma against hydrogen peroxide. *Asian Pac. J. Trop. Biomed.* **2011**, *1*, 57–63. [[CrossRef](#)]

55. Lopez-Novoa, J.M.; Quiros, Y.; Vicente, L.; Morales, A.I.; Lopez-Hernandez, F.J. New insights into the mechanism of aminoglycoside nephrotoxicity: An integrative point of view. *Kidney Int.* **2011**, *79*, 33–45. [[CrossRef](#)]
56. Quiros, Y.; Vicente-Vicente, L.; Morales, A.I.; López-Novoa, J.M.; López-Hernández, F.J. An integrative overview on the mechanisms underlying the renal tubular cytotoxicity of gentamicin. *Toxicol. Sci.* **2011**, *119*, 245–256. [[CrossRef](#)]
57. Mestry, S.N.; Gawali, N.B.; Pai, S.A.; Gursahani, M.S.; Dhodi, J.B.; Munshi, R.; Juvekar, A.R. Punica granatum improves renal function in gentamicin-induced nephropathy in rats via attenuation of oxidative stress. *J. Ayurveda Integr. Med.* **2020**, *11*, 16–23. [[CrossRef](#)]
58. Nitha, B.; Janardhanan, K. Aqueous-ethanolic extract of morel mushroom mycelium *Morchella esculenta*, protects cisplatin and gentamicin induced nephrotoxicity in mice. *Food Chem. Toxicol.* **2008**, *46*, 3193–3199. [[CrossRef](#)]
59. Farombi, E.; Ekor, M. Curcumin attenuates gentamicin-induced renal oxidative damage in rats. *Food Chem. Toxicol.* **2006**, *44*, 1443–1448. [[CrossRef](#)]
60. Zroui, H.; Elbouzidi, A.; Bouhrim, M.; Bencheikh, N.; Kharchoufa, L.; Ouahhoud, S.; Ouassou, H.; El Assri, S.; Choukri, M. Phytochemical analysis, antioxidant activity, and nephroprotective effect of the *Raphanus sativus* aqueous extract. *Mediterr. J. Chem.* **2021**, *11*, 84–94. [[CrossRef](#)]

Disclaimer/Publisher’s Note: The statements, opinions and data contained in all publications are solely those of the individual author(s) and contributor(s) and not of MDPI and/or the editor(s). MDPI and/or the editor(s) disclaim responsibility for any injury to people or property resulting from any ideas, methods, instructions or products referred to in the content.